

## Supporting Information

### Selective ion sieving through arrays of sub-nanometer nanopores in chemically tunable 2D carbon membranes

**Authors:** Pauline M. G. van Deursen, Zian Tang, Andreas Winter, Michael J. Mohn, Ute Kaiser, Andrey A. Turchanin, Grégory F. Schneider

#### Contents:

- Figure S1: Equivalent circuit for measurement of  $G_{\text{CNM}}$
- Table S2: Activity coefficients and definition of  $V_{\text{Nernst}}$
- Figure S3: Survey XP spectra of BPT-SAM and BPT-CNM on gold/mica
- Figure S4: High resolution XP spectra of BPT-SAM and BPT-CNM on gold/mica

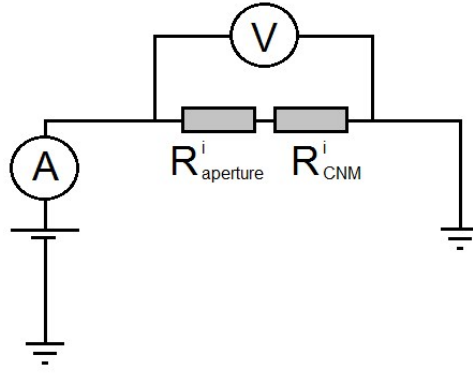


**Figure S1:** Equivalent circuit of the CNM-coated  $\text{Si}_3\text{N}_4$  aperture in the current-voltage measurement. To obtain the conductance of the BPT-CNM from the measured  $I(V)$  curves,

the resistance of each CNM-coated  $\text{Si}_3\text{N}_4$  aperture was determined as  $R_{measured}^i = \frac{V}{I}$ . The measured resistance is the sum of the contributions from the  $\text{Si}_3\text{N}_4$  aperture and the CNM. To account for this, the resistance that was recorded before membrane deposition (red data points in Figure 2a) is subtracted from the measured resistance:  $R^i = R_{measured}^i - R_{SiN}^i$ . The

conductance of the CNM samples, then, is  $G^i = \frac{1}{R^i}$ . The conductance of the BPT-CNM membrane is determined by taking the average value of the conductance measured on each sample:  $G_{CNM} = \langle G^i \rangle$ .

**Table S2.** Activity coefficients of electrolytes used in the measurements of ion selective transport.<sup>1</sup>

$\gamma$ C (mol/kg)	KCl	CsCl	MgCl <sub>2</sub>
0.1	0.768	0.751	0.535
1	0.604	0.546	0.577

The theoretical maximum membrane potential was calculated using Nernst equation:<sup>2</sup>

$$V_{Nerst} = \frac{RT}{FZ} \ln \left( \frac{\gamma_{C\ high} C_{high}}{\gamma_{C\ low} C_{low}} \right)$$

where R is the universal gas constant, T is the temperature, F Faradays constant and Z the valency of the electrolyte, C the electrolyte concentration on either side of the membrane and  $\gamma$  the electrolyte activity coefficient as tabulated above.

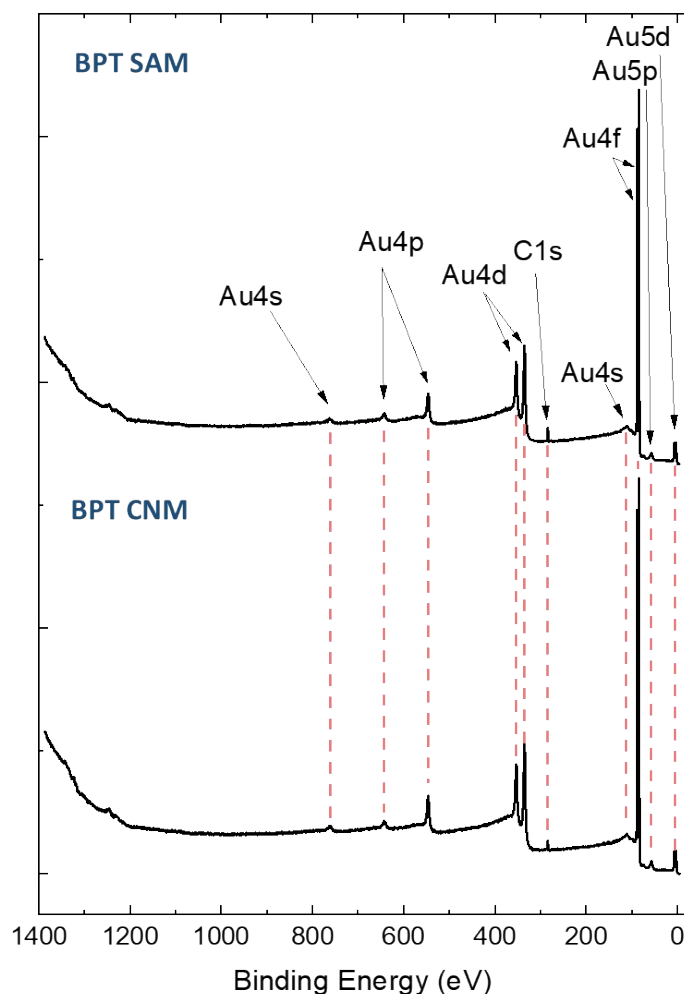


**Figure S3:** Elemental analysis of the BPT-CNM based on XP survey spectra of BPT-SAM before cross-linking into a covalent membrane, and of the BPT-CNM after cross-linking. XPS measurements were done on the BPT-SAM and the BPT-CNM on Au/mica substrates. The Au4f<sub>7/2</sub> (84.0 eV) peak was used for the binding energy calibration. The red dashed line are included to guide the eye to the respective XP peaks in both samples. The C1s peak indicates the presence of carbon.

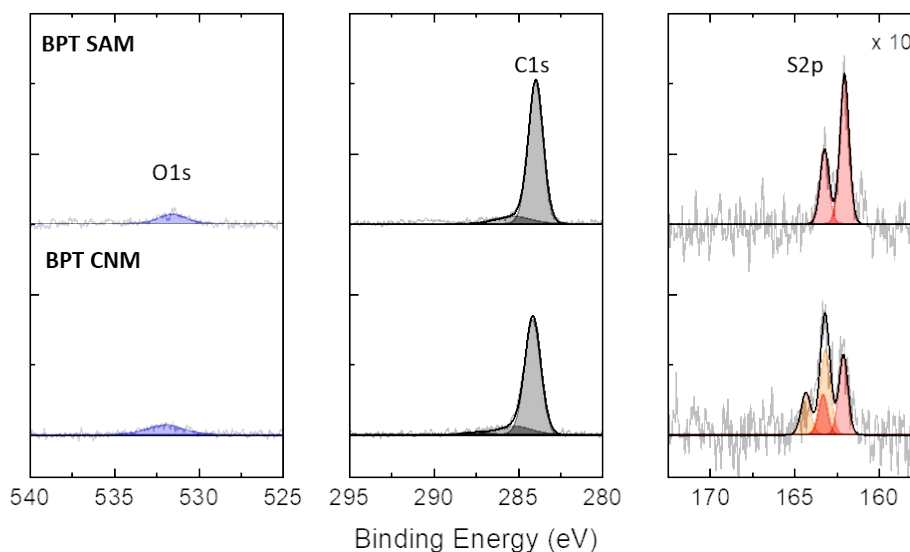


**Figure S4:** High-resolution XP spectra of BPT-SAM and BPT-CNM on gold/mica substrates including the S2p, C1s and O1s signals. For better visualization, the intensity of the S2p peak is multiplied by a factor of 10. The spectra were fitted employing the Voigt functions with Gaussian-Lorentzian ratio of 80:20 and after subtraction of the Shirley background. As expected<sup>3,4</sup> the C1s signal of the BPT-SAM consist of a main aromatic peak at 284.0 eV accompanied by a smaller shoulder at 285.3 eV due to C-S bonds. The S2p signal is the characteristic thiolate doublet with the binding energies (BEs) of S2p<sub>3/2</sub> and S2p<sub>1/2</sub> at 162.0 eV and 163.2 eV, respectively, and the I(S2p<sub>3/2</sub>):I(S2p<sub>1/2</sub>) intensity ratio of 2:1. After the formation of a BPT-CNM, the C1s peak widens and its intensity decreases by ~10% and a new S2p doublet at BEs of 163.2 eV and 164.4 eV for S2p<sub>3/2</sub> and S2p<sub>1/2</sub>, respectively, forms. Both changes are due to the formation of covalently bond network out of the SAM.<sup>3,4</sup> As the samples were transferred to the ultra-high vacuum XPS chamber from ambient conditions, a small amount of airborne contaminations (O1s peak) can be recognized on the surface of both samples.

## References

- 1 David R. Lide, Ed., *CRC Handbook of Chemistry and Physics*, CRC Press LLC, Boca Raton, 80th edn., 1999.
- 2 Sata, T. *Ion exchange membranes: preparation, characterization, modification and application*. Royal Society of Chemistry, Cambridge, 2007: pp 13–16.
- 3 A. Turchanin, D. Käfer, M. El-Desawy, C. Wöll, G. Witte and A. Götzhäuser, *Langmuir*, 2009, **25**, 7342–7352.
- 4 P. Angelova, H. Vieker, N. Weber, D. Matei, O. Reimer, I. Meier, S. Kurasch, J. Biskupek, D. Lorbach, K. Wunderlich, L. Chen, A. Terfort, M. Klapper, K. Müllen, U. Kaiser, A. Götzhäuser and A. Turchanin, *ACS Nano*, 2013, **7**, 6489–6497.